



Article

Visible Light-Assisted Photocatalysis Using Spherical-Shaped BiVO₄ Photocatalyst

Yuvaraj M. Hunge¹, Akihiro Uchida^{1,2}, Yusuke Tominaga^{1,2}, Yuta Fujii^{1,2}, Anuja A. Yadav³, Seok-Won Kang³, Norihiro Suzuki¹ , Isao Shitanda^{1,2}, Takeshi Kondo^{1,2}, Masayuki Itagaki², Makoto Yuasa^{1,2}, Suresh Gosavi^{1,4}, Akira Fujishima¹ and Chiaki Terashima^{1,*} 

- ¹ Photocatalysis International Research Center, Research Institute for Science and Technology, Tokyo University of Science, 2641 Yamazaki, Noda, Chiba 278-8510, Japan; yuvihunge@gmail.com (Y.M.H.); 7219513@ed.tus.ac.jp (A.U.); 7220552@ed.tus.ac.jp (Y.T.); 7220564@ed.tus.ac.jp (Y.F.); suzuki.norihiro@rs.tus.ac.jp (N.S.); shitanda@rs.tus.ac.jp (I.S.); t-kondo@rs.tus.ac.jp (T.K.); yuasa@rs.tus.ac.jp (M.Y.); swg@physics.unipune.ac.in (S.G.); fujishima_akira@admin.tus.ac.jp (A.F.)
- ² Department of Pure and Applied Chemistry, Faculty of Science and Technology, Tokyo University of Science, 2641 Yamazaki, Noda, Chiba 278-8510, Japan; itagaki@rs.tus.ac.jp
- ³ Department of Automotive Engineering, Yeungnam University, 280 Daehak-ro, Gyeongsan, Gyeongbuk 38541, Korea; anujayadav5@yu.ac.kr (A.A.Y.); swkang@yu.ac.kr (S.-W.K.)
- ⁴ Center for Advance Studies in Material Science and Solid State Physics, Department of Physics, Savitribai Phule Pune University, (Formerly University of Pune), Pune 411 007, India
- * Correspondence: terashima@rs.tus.ac.jp; Tel.: +81-4-7124-1501



Citation: Hunge, Y.M.; Uchida, A.; Tominaga, Y.; Fujii, Y.; Yadav, A.A.; Kang, S.-W.; Suzuki, N.; Shitanda, I.; Kondo, T.; Itagaki, M.; et al. Visible Light-Assisted Photocatalysis Using Spherical-Shaped BiVO₄ Photocatalyst. *Catalysts* **2021**, *11*, 460. <https://doi.org/10.3390/catal11040460>

Academic Editor: Vincenzo Vaiano

Received: 11 March 2021

Accepted: 30 March 2021

Published: 1 April 2021

Publisher's Note: MDPI stays neutral with regard to jurisdictional claims in published maps and institutional affiliations.



Copyright: © 2021 by the authors. Licensee MDPI, Basel, Switzerland. This article is an open access article distributed under the terms and conditions of the Creative Commons Attribution (CC BY) license (<https://creativecommons.org/licenses/by/4.0/>).

Abstract: In this research work, we reported the synthesis of a spherical-shaped bismuth vanadate (BiVO₄) photocatalyst using a cost-effective, simple, chemical hydrothermal method and studied the effect of deposition temperatures on the structural, morphological, optical properties, etc. The XRD result confirmed the monoclinic scheelite phase of BiVO₄. An XPS study confirmed the occurrence of Bi, V, and O elements and also found that Bi and V exist in +3 and +5 oxidation states, respectively. SEM micrographs revealed the spherical-shaped morphology of the BiVO₄ photocatalyst. Optical investigation showed that the bandgap of the BiVO₄ photocatalyst varied between 2.25 and 2.32 eV. The as-synthesized BiVO₄ photocatalyst was used to study the photocatalytic degradation of crystal violet (CV) dye under visible light illumination. The photocatalytic degradation experiment showed that the degradation percentage of crystal violet dye using BiVO₄ reached 98.21% after 120 min. Mineralization of crystal violet dye was studied using a chemical oxygen demand analysis.

Keywords: hydrothermal method; BiVO₄; photocatalysis; crystal violet dye

1. Introduction

In recent decades, the semiconductor-assisted photocatalysis process has proven to be effective for the decomposition of organic pollutants, such as acids, dyes, and aromatic and phenolic compounds, etc., which are present in wastewater, due to its strong redox potential, environmental friendliness, moderate operation temperature, easy operation, and useful final products [1,2]. In recent years, researchers have tried to develop novel photocatalyst materials that are visible light-responsive due to their stability, modifiable energy band structure, low cost, non-toxicity, and environmental friendliness. Presently, several visible light-responsive photocatalysts, such as BiVO₄, g-C₃N₄, and Ag₃PO₄, etc., have been developed and used in the photocatalytic destruction of organic pollutants. Among the different visible light-responsive photocatalysts, BiVO₄ is one of the better, n-type visible light-driven photocatalysts, which has received much attention due to its narrow bandgap, non-toxicity, favorable valence band position, and high stability during the photocatalytic reaction [3–5]. It has been used in different applications such as supercapacitors, gas sensors, batteries, hydrogen production, photocatalysis, etc. Furthermore, it is used as a pigment and a ferroelectric material. It occurs in three major crystal phases, namely

monoclinic scheelite, tetragonal zircon, and tetragonal scheelite [6,7]. Among these, the monoclinic BiVO_4 phase has a bandgap energy of 2.4 eV, making it the most appropriate BiVO_4 phase for visible light-induced photocatalysis applications [8].

Different methods have been reported for the synthesis of BiVO_4 photocatalyst such as solid-state reaction, sonochemical, organic decomposition, precipitation, hydrothermal, sol-gel, etc. [9]. Among these, the hydrothermal method is considered to be a good technological process for preparing photocatalysts. There are several advantages of the hydrothermal method such as lower deposition temperatures, high purity of materials, good control of the size and shape of the particles, and the opportunity to obtain good crystalline material in a single step without post-annealing treatment, etc. [10]. Furthermore, this method is useful to produce different morphologies of the BiVO_4 photocatalyst such as flower-like, flake-like, cuboid-like, and plate-like structures, etc., in order to improve the specific surface area and the photodegradation efficiency [11].

Kudo et al. [12] prepared highly crystalline monoclinic and tetragonal BiVO_4 using an aqueous process via reaction of the layered potassium vanadates KV_3O_8 and $\text{K}_3\text{V}_5\text{O}_{14}$ with $\text{Bi}(\text{NO}_3)_3$ at 20 °C for three days. Guo et al. [13] made a BiVO_4 catalyst using a facile surfactant-free method and studied the photocatalytic degradation of methylene blue. Sarkar et al. [14] prepared a spherical-shaped BiVO_4 photocatalyst using a precursor-mediated growth method and investigated the photocatalytic degradation of Rhodamine B under visible light illumination. Dong et al. [15] synthesized sponge-like BiVO_4 films prepared with polystyrene (PS) as a pore-forming material and F-doped SnO_2 (FTO) glass as a substrate and reported photoelectrocatalytic degradation of phenol under visible light irradiation. Deebasree et al. [16] synthesized a BiVO_4 photocatalyst using a sol-gel-assisted ultrasonication method by varying the output power and studied the decolorization of methylene blue under visible light irradiation. Chen et al. [17] fabricated a BiVO_4 photocatalyst using a microwave hydrothermal process and studied the overall water-splitting reaction.

Herein, we reported the preparation of a spherical-shaped BiVO_4 photocatalyst using a simple, chemical, cost-effective hydrothermal method. Furthermore, we studied the effect of different deposition temperatures on the structural, morphological, optical, and photocatalytic properties of the BiVO_4 photocatalyst. The prepared catalyst materials were characterized using different characterization tools such as X-ray diffraction (XRD), Raman spectroscopy, X-ray photoelectron spectroscopy (XPS), scanning electron microscopy (SEM), and UV-Vis spectroscopy, etc. Crystal violet (CV) dye is used in many industries such as the textile, paper, agriculture, and leather industries. Therefore, it was chosen as the model organic impurity in order to evaluate the photocatalytic performance of the spherical-shaped BiVO_4 photocatalyst under visible light illumination. Crystal violet was successfully degraded using the BiVO_4 photocatalyst without the use of external catalysts, such as H_2O_2 , HClO_4 , and NaH_2PO_4 , etc., which influence the degradation efficiency. Furthermore, we obtained good degradation efficiency compared to the literature (Table 1).

2. Results and Discussion

The crystal structures of the as-synthesized BiVO_4 samples were studied using XRD. Figure 1 presents the XRD patterns of the BiVO_4 photocatalysts synthesized at different deposition temperatures. The XRD patterns were measured by varying the diffraction angle (2θ) from 10° to 70°. All of the prepared samples were polycrystalline. For all of the synthesized photocatalysts, the diffraction peaks were well indexed to the monoclinic scheelite phase of BiVO_4 (JCPDS Card number 01-083-1699) [18]. As the deposition temperature increased from 140 to 160 °C, the intensity of the (1 2 1) plane increased and then decreased with a further increase in deposition temperature. The BiVO_4 sample deposited at 160 °C was highly crystalline and the preferred orientation was observed along the (1 2 1) plane for all samples. A higher intensity indicated a higher extent of crystallization along that plane [19]. The average crystallite size was calculated using Debye-Scherrer's formula and was found to be 28.81, 26.90, and 27.68 nm for samples prepared at temperatures

of 140, 160, and 180 °C, respectively. No impurity peaks or mixed phases were detected. Furthermore, confirmation of the formation of the BiVO₄ photocatalysts was achieved using Raman spectroscopy.

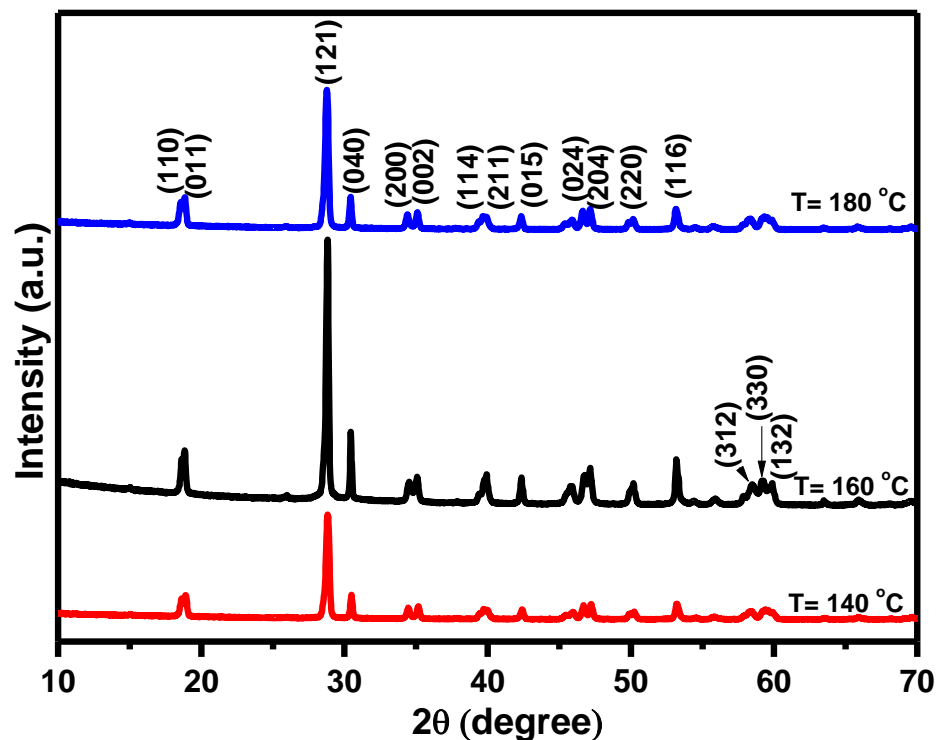


Figure 1. XRD patterns of BiVO₄ photocatalysts prepared at different deposition temperatures.

Raman spectroscopy is a useful characterization tool to understand the local structure and symmetry of a material. Figure 2 shows the Raman spectra of the BiVO₄ photocatalysts. From the Raman spectra, it is evident that there are four well-resolved characteristic peaks (199.85, 315.10, 355.75, and 813.12 cm⁻¹) with different intensities. A similar trend was observed in the Raman study to that seen in the XRD result. The maximum peak intensity was observed for the sample prepared at 160 °C. The occurrence of a peak at 813.12 cm⁻¹ corresponds to the symmetric V-O stretching mode (Ag symmetry) [20], while the other peaks at 315.10 and 355.75 cm⁻¹ are attributed to the bending modes of the VO₄ tetrahedra [21], and the peak at 199.85 cm⁻¹ corresponds to the vibration of the crystal lattice [22]. The Raman and XRD results confirm the formation of the monoclinic scheelite phase of the BiVO₄ photocatalysts.

An XPS study was used to investigate the chemical composition and oxidation states that the BiVO₄ photocatalyst deposited at 160 °C and they are presented in Figure 3. Figure 3a presents the survey scan spectrum of the BiVO₄ photocatalyst, which shows that the sample was composed of Bi, V, and O elements and no other impurity elements were found. The Bi 4f spectrum is shown in Figure 3b. The peaks located at binding energies of 159.28 and 164.60 eV correspond to Bi 4f_{7/2} and Bi 4f_{5/2}, respectively [23]. This result proves that Bi exists in the +3 oxidation state. Figure 3c displays the V 2p spectrum, which splits into two major peaks at binding energy values of 516.75 (V 2p_{3/2}) and 524.60 eV (V 2p_{1/2}) that were assigned to V⁵⁺ [24]. Figure 3d presents the high-resolution O 1s spectra of the BiVO₄ photocatalyst, which were fitted into two components at binding energy values of 530.40 and 532.15 eV, which are signals from the hydroxyl group and adsorbed water on the surface of the catalyst [25].

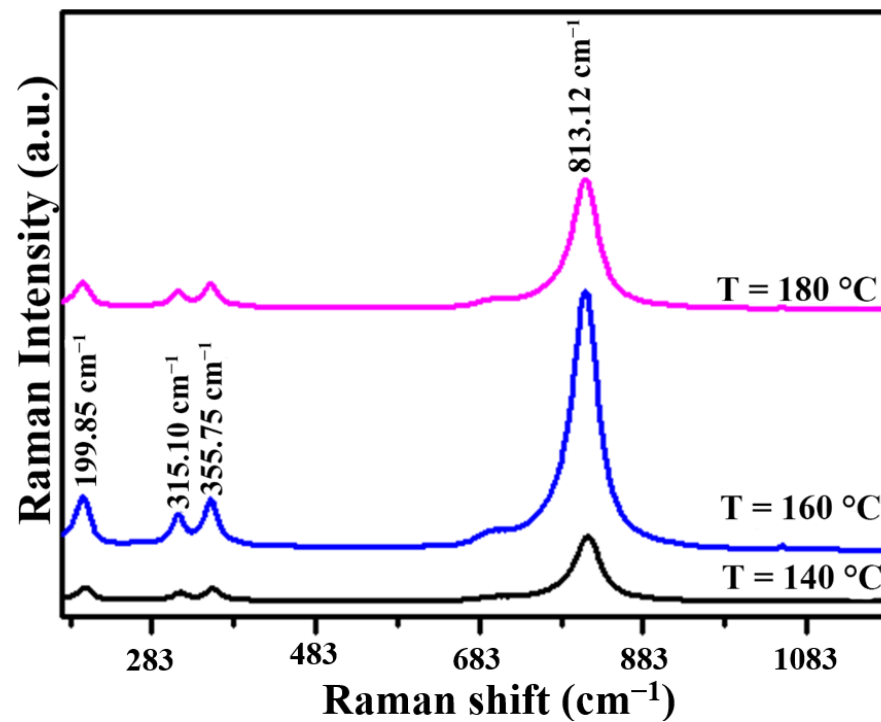


Figure 2. Raman spectra of BiVO_4 photocatalysts prepared at different deposition temperatures.

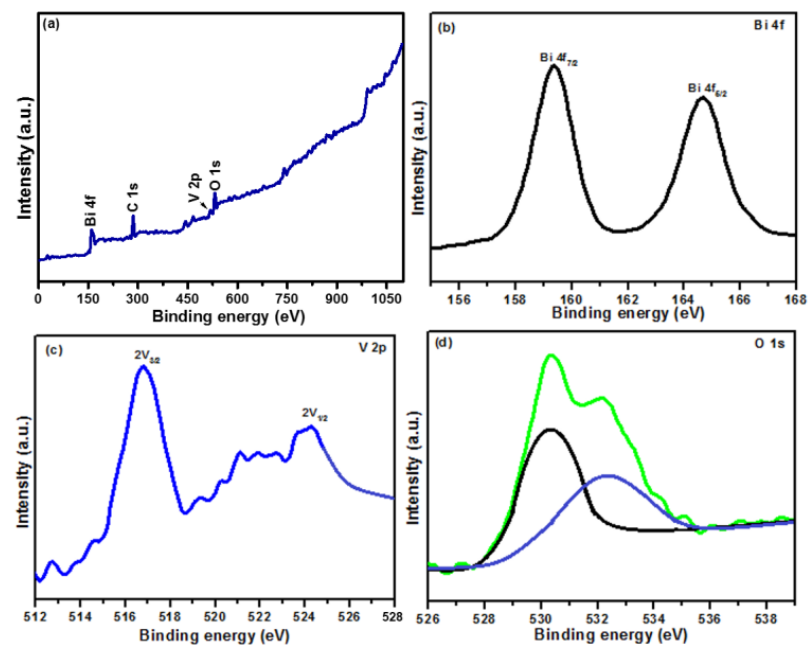


Figure 3. XPS spectra of BiVO_4 photocatalyst deposited at $160\text{ }^\circ\text{C}$: (a) narrow scan spectrum; (b) Bi 4f, (c) V 2p, and (d) O 1s spectra.

Surface morphology plays a crucial role in photocatalysis application. The morphology of the prepared BiVO_4 photocatalysts was characterized using scanning electron microscopy. Figure 4a–c display SEM micrographs of the BiVO_4 photocatalyst prepared at a $160\text{ }^\circ\text{C}$ deposition temperature. From the first SEM image (Figure 4a), spherical-shaped BiVO_4 particles with agglomeration in some places are evident [26]. Figure 4b,c present SEM micrographs at a higher magnification. Such spherical-shaped morphology is useful for photocatalysis application [27].

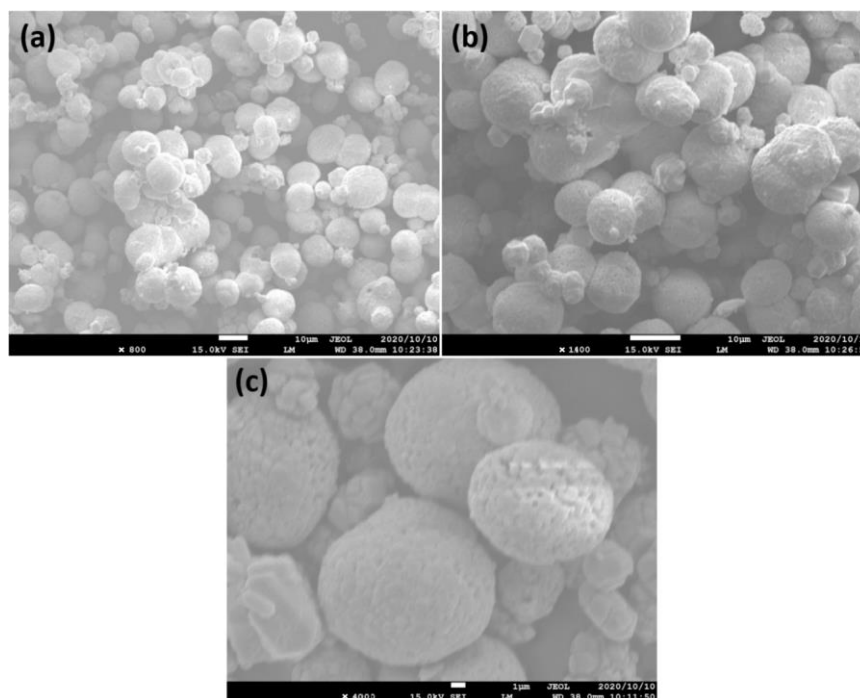


Figure 4. (a–c) SEM images of BiVO_4 photocatalyst deposited at 160°C with different magnifications.

Optical study is an important characterization technique for studying photocatalysis application. Therefore, we employed UV–Vis spectroscopy to determine the absorption edges and bandgap energy of the BiVO_4 photocatalysts. Figure 5a,b present the UV–Vis absorbance spectra and bandgap plot, respectively, of the BiVO_4 photocatalysts at different deposition temperatures. Absorbance spectra were measured in the wavelength range of 300–800 nm. The bandgap edges of the BiVO_4 photocatalysts were estimated at 645 (140°C), 660 (160°C), and 636 nm (180°C). It was observed that all BiVO_4 samples had stronger and wider absorption in the visible region. Figure 5b displays the bandgap plot of the BiVO_4 samples. By plotting the graph of $(\alpha h\nu)^n$ versus $h\nu$ for the BiVO_4 photocatalysts, the bandgap was determined. The bandgap was determined by plotting a tangent line across the vertical part of the curve and intersecting it with a horizontal reference line [28]. The bandgap energy for the BiVO_4 photocatalysts was found to be 2.32 (140°C), 2.25 (160°C), and 2.28 eV (180°C).

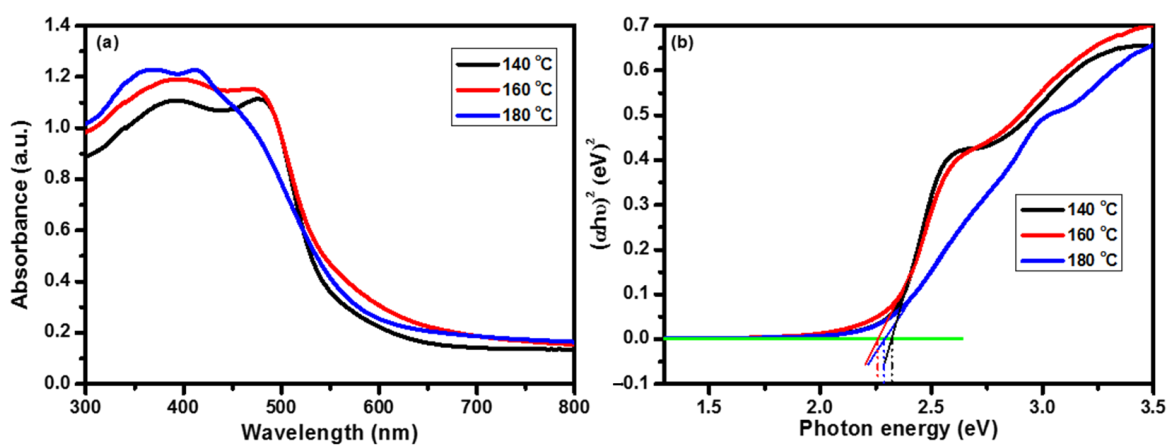


Figure 5. (a) Absorbance spectra and (b) bandgap plot for BiVO_4 photocatalysts deposited at different deposition temperatures.

Figure 6 shows the photoluminescence (PL) spectra of the BiVO_4 photocatalysts. PL spectra provide useful information about the migration, transfer, and recombination

processes of the photogenerated charge carriers (electron–hole pairs) in semiconductor materials. The intensity of PL emission peaks is associated with the recombination of photogenerated electrons and holes. Therefore, a low-intensity PL emission peak implies a lower recombination of charge carriers upon light irradiation, and vice versa [29,30]. A broad emission peak was observed around 577 nm. The sample deposited at 160 °C exhibited the lowest PL intensity in the range of 540–610 nm compared to the BiVO₄ samples deposited at 140 and 180 °C. These results show that the sample deposited at 160 °C had the lowest recombination of photogenerated charge carriers. The XRD, Raman, UV–Vis, and PL results proved that the sample deposited at 160 °C was better for studying the photocatalytic activity because the sample deposited at 160 °C had good crystallinity, lower recombination of photogenerated charge carriers, etc.

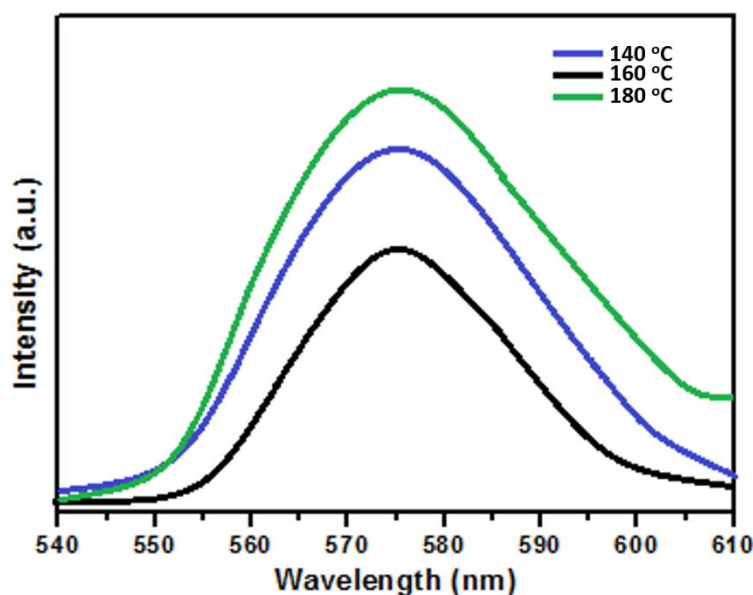


Figure 6. Photoluminescence (PL) spectra of BiVO₄ photocatalysts deposited at different deposition temperatures.

3. Photocatalytic Degradation Activity and Stability Performance

The photocatalytic performance of the BiVO₄ photocatalyst prepared at 160 °C was used to study the degradation of crystal violet dye under visible light irradiation and the results are presented in Figure 7. Figure 7a displays the extinction spectra of crystal violet dye collected at different time intervals. The extinction spectra were recorded in the wavelength range 400–700 nm. A strong absorption peak was observed at 590 nm for the crystal violet dye [31]. From the extinction spectra, it was observed that the maximum absorbance at 590 nm decreased gradually and eventually disappeared after 120 min, indicating oxidative degradation of the crystal violet dye. During the progress of the degradation experiments, the frequent decrease in the extinction indicated a decrease in the crystal violet dye concentration with respect to time, and it was also visually confirmed by the reaction solution decoloration. This observation confirms that a redox reaction taking place on the surface of BiVO₄ photocatalyst [32]. From this plot, degradation percentage was calculated. The following equation was used to calculate the degradation percentage [33].

$$\text{Degradation efficiency} = \frac{C_0 - C}{C_0} \times 100(\%) \quad (1)$$

where C and C_0 are the final and initial concentrations of crystal violet dye, respectively. It was found that 98.21% degradation of CV dye occurs under visible light illumination. Using the extinction plot, the graph of $\ln(C/C_0)$ vs. reaction time was plotted and is shown

in Figure 7b. From the slope, the plot's reaction rate constant was calculated. Equation (2) was used to calculate the rate constant of the reaction [34].

$$\ln\left(\frac{C}{C_0}\right) = -k \cdot t \quad (2)$$

where t is the time and k can be taken as the apparent first-order rate constant of the degradation reaction. The value of the rate constant k was found to be $5.88 \times 10^{-6} \text{ s}^{-1}$. The variation in chemical oxygen demand (COD) values with respect to reaction time when using the BiVO_4 photocatalyst is presented in Figure 7c. Unlike extinction, studying COD as a function of illumination time gives information about the concentration of oxidizable matter left in the electrolyte solution, not the concentration of the parent molecule. From the graph, it can be observed that the values of COD decrease with the increase in reaction time. COD values decreased from 78.1 to 7.4 mg/L. The variation in COD values indicates that the rate of degradation was high in the initial period, followed by a slow rate. This slow rate indicates the formation of a few long-lived intermediate by-products, which have a low reaction rate with hydroxyl radicals, which revealed the formation of intermediates such as aldehydes and aliphatic acids, etc. [35]. These intermediate products proceeded at a much slower reaction rate; therefore, the reduction in COD values resulted from the degradation of the CV dye.

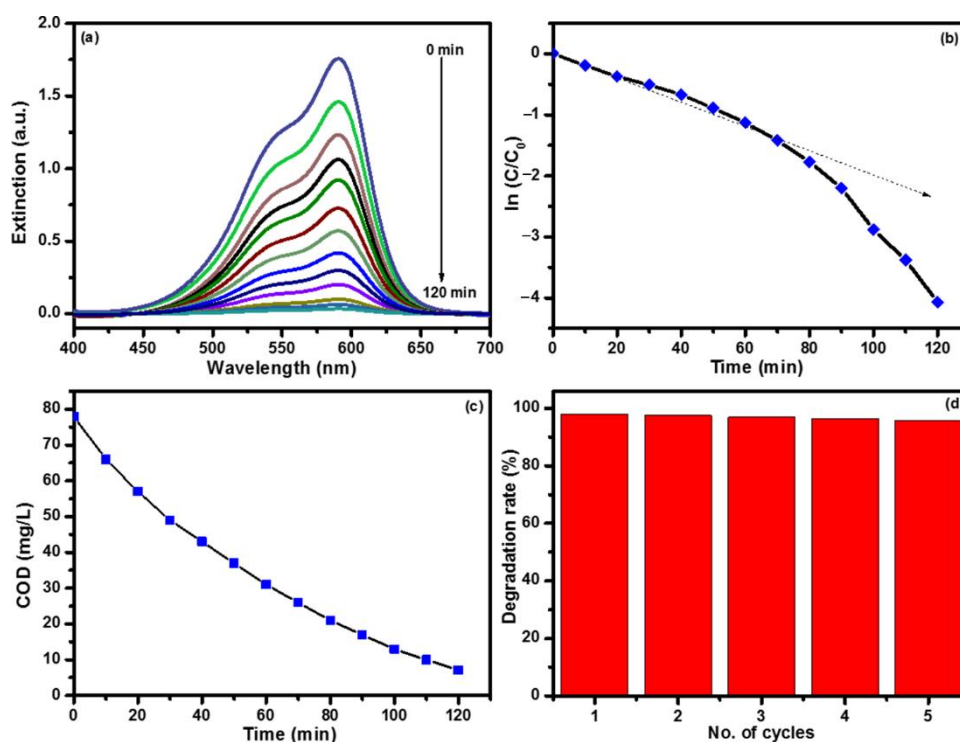


Figure 7. Photocatalytic degradation of crystal violet dye using BiVO_4 photocatalyst prepared at 160°C temperature. (a) Extinction spectra; (b) $\ln(C/C_0)$ vs. reaction time; (c) variation in chemical oxygen demand (COD) values of crystal violet dye with respect to reaction time, and (d) stability study.

The stability study of a photocatalyst is an important factor for its practical applications. Therefore, the photostability of the sample synthesized at 160°C was evaluated in repeated photocatalytic experiments under similar experimental conditions. To study the stability of the as-prepared BiVO_4 photocatalyst, degradation experiments were performed and the stability was checked five times with the same BiVO_4 photocatalyst. The stability study showed that little decrease was observed in the degradation efficiency after five successive runs, as shown in Figure 7d. There were no noticeable changes in the degradation

percentage of the CV dye. However, a slight decrease in the degradation percentage was observed, which may have been due to the loss of catalyst during centrifugation [36]. A 98.21% photocatalytic degradation efficiency was observed for the first time, which slightly reduced to 95.80% after the fifth cycle run. Thus, the BiVO₄ catalyst exhibited good stability and recyclability for CV dye degradation. Table 1 presents the photocatalytic degradation of crystal violet dye using different materials and methods.

Table 1. Photocatalytic degradation of crystal violet (CV) dye using different materials and methods.

Sr. No.	Materials	Methods	Degradation Percentage (Time)	References
1	ZnO	Chemical solution route	88.84% (7 h)	[37]
2	GO	Chemical solution route	97.90% (24 h)	[37]
3	ZnO/GO	Co-precipitation	99% (240 min)	[38]
4	BiVO ₄	Hydrothermal	96.23% (120 min)	[39]
5	BiVO ₄	Hydrothermal	98.21% (120 min)	Present work

Figure 8 presents the possible pathways for photocatalytic degradation of crystal violet dye using the BiVO₄ photocatalyst under visible light illumination. Initially, oxidized intermediate products were formed, which involved the N-demethylation of the CV dye and the cleavage of the chromosphere structure, which occurred due to the loss of aromatic conjugation and after the hydroxylation of intermediates. Hydroxylated species were oxidized to the quinoid compound, while in the second step, the aromatic rings opened and carboxylic acids were formed. The ring-opening processes continued and the final degradation products could be CO₂ and H₂O. The latter situation is achieved only when the degradation process reaches mineralization [32,40].

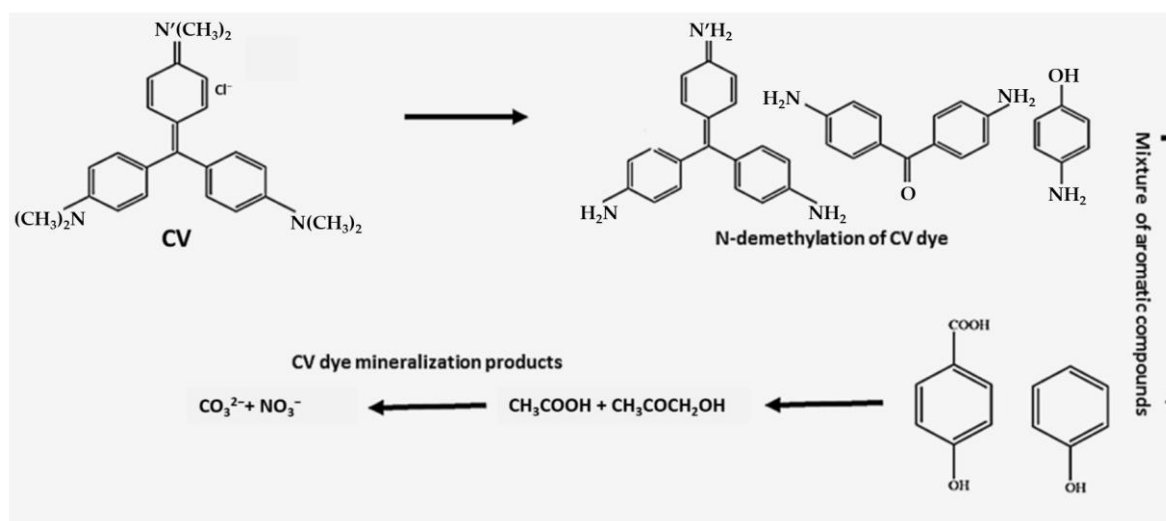


Figure 8. Possible pathways for photocatalytic degradation of crystal violet using BiVO₄ photocatalyst under visible light illumination.

4. Materials and Methods

4.1. Materials

All chemicals were purchased from commercial sources and used without further purification. Bismuth nitrate pentahydrate (Bi(NO₃)₃·5H₂O), ammonium metavanadate (NH₄VO₃), sodium hydroxide (NaOH), potassium dichromate (K₂Cr₂O₇), sulfuric acid (H₂SO₄), and nitric acid (HNO₃) were purchased from Sigma-Aldrich.

4.2. Preparation of BiVO₄ Photocatalysts

BiVO₄ photocatalysts were prepared using the hydrothermal method. In a typical synthesis process, firstly, solution A was prepared by dissolving 2 mmol of Bi(NO₃)₃·5H₂O in a concentrated nitric acid solution under constant stirring. Solution B was prepared by dissolving 2 mmol (NH₄VO₃) in a sodium hydroxide solution. Then, solutions A and B were mixed together well under vigorous stirring and the pH of this solution was adjusted to 7 using NaOH solution (1 M). Lastly, the obtained mixed solution was transferred into a 50-mL Teflon-lined stainless steel autoclave and kept in a furnace at different deposition temperatures of 140, 160, and 180 °C for 12 h. The formed precipitate was collected, filtered, washed with distilled water several times, and then dried in a vacuum at 80 °C for 6 h. The BiVO₄ photocatalysts prepared using this method had good morphology, stability, and high purity.

4.3. Material Characterization

The structural, morphological, and optical properties of the prepared BiVO₄ catalysts were investigated using several characterization techniques. The structural properties were analyzed using X-ray diffraction (XRD; Ultima IV, Rigaku, Tokyo, Japan) and Raman scattering spectroscopy (NRS-5100, JASCO, Tokyo, Japan). The XPS analysis of the catalyst was carried out using an AXIS Nova X-ray photoelectron spectrometer (Milton Keynes, UK). The surface morphology was analyzed using scanning electron microscopy (SEM; JSM-7600F, JEOL, Tokyo, Japan). The optical properties were studied using photoluminescence (PL), photoluminescence excitation (PLE) spectroscopy (LS5, Perkin Elmer, Waltham, MA, USA), and UV–Vis absorption spectroscopy (V-670, JASCO, Japan).

4.4. Photocatalytic Activity

The photocatalytic activity of the as-prepared BiVO₄ photocatalyst was evaluated through the degradation of crystal violet dye under visible light irradiation at room temperature. An amount of 0.5 mM of crystal violet dye was used as the model organic impurity. A 300-W Xe lamp ($\lambda > 420$ nm) was used as the visible light source and a 420-nm cut-off filter was placed between the lamp and the reaction mixture to filter out UV light. In the actual experiment, 0.2 g of catalyst was dispersed into a beaker containing 200 mL of 0.5 mM crystal violet aqueous solution. This mixture was magnetically stirred in the dark for 30 min before illumination in order to attain an adsorption/desorption equilibrium. Then, the reaction solution was exposed to visible light illumination whilst under constant magnetic stirring. At specific time intervals, 3 mL of the reaction solution was collected and centrifuged. After centrifugation, the reaction solution was analyzed using a UV–Vis spectrophotometer.

Samples (0.8 mL) withdrawn from the reaction mixture at different time intervals during the photocatalytic degradation experiment were also used to determine the chemical oxygen demand (COD). The samples (0.8 mL) withdrawn at different time intervals were mixed with an excess of potassium dichromate (0.7 mL) and sulfuric acid (2 mL), and the mixture was heated under total reflux conditions for a period of two hours at 140 °C. During the reaction, the chemically oxidizable organic material reduced a stoichiometrically equivalent quantity of dichromate. The quantity of potassium dichromate reduced gave a measure of the amount of oxidizable organic material. From the dichromate extinction, the concentration of the organic solute was calculated [41].

5. Conclusions

A BiVO₄ photocatalyst was successfully prepared using the hydrothermal method. The effect of different deposition temperatures on the structural and optical properties of the BiVO₄ photocatalyst was studied. The XRD, Raman, and PL results confirmed that the sample prepared at 160 °C was considered to be the optimized sample. The XRD and Raman results confirmed the formation of BiVO₄. The SEM study revealed the spherical-shaped morphology of the BiVO₄ photocatalyst. Optical investigation showed that the

BiVO₄ catalyst has strong absorption in the visible region. The chief vibrational modes of the BiVO₄ sample, located at 315.10, 355.75, and 813.12 cm⁻¹ and corresponding to the bending and symmetric stretching modes of vibration, were consistent with the monoclinic structure. The photocatalytic degradation percentage of crystal violet dye reached up to 98.21% with good photostability when using the BiVO₄ photocatalyst under visible light illumination. The extent of mineralization of the degraded sample was confirmed using a chemical oxygen demand analysis.

Author Contributions: Y.M.H., A.U., Y.T., Y.F., A.A.Y. and S.-W.K.: data curation, formal analysis, investigation, writing—original draft. N.S., I.S., T.K., M.L., M.Y. and S.G.: investigation, methodology. A.F.: conceptualization, project administration, supervision. C.T.: project administration, supervision, conceptualization, methodology. All authors have read and agreed to the published version of the manuscript.

Funding: This study was partly supported by the MEXT Promotion of Distinctive Joint Research Center Program Grant Number JPMXP0618217662.

Institutional Review Board Statement: Not applicable.

Informed Consent Statement: Not applicable.

Data Availability Statement: Data are contained within the article.

Conflicts of Interest: The authors declare no conflict of interest.

References

1. Hu, J.; Chen, D.; Li, N.; Xu, Q.; Li, H.; He, J.; Lu, J. In Situ fabrication of Bi₂O₂CO₃/MoS₂ on carbon nanofibers for efficient photocatalytic removal of NO under visible-light irradiation. *Appl. Catal. B-Environ.* **2017**, *217*, 224–231. [[CrossRef](#)]
2. Liu, J.; Liu, Y.; Liu, N.; Han, Y.; Zhang, X.; Huang, H.; Kang, Z. Metal-free efficient photocatalyst for stable visible water splitting via a two-electron pathway. *Science* **2015**, *347*, 970–974. [[CrossRef](#)] [[PubMed](#)]
3. Chang, X.X.; Wang, T.; Zhang, P.; Zhang, J.J.; Li, A.; Gong, J.L. Enhanced surface reaction kinetics and charge separation of p-n heterojunction CO₃O₄/BiVO₄ photoanodes. *J. Am. Chem. Soc.* **2015**, *137*, 8356–8359. [[CrossRef](#)]
4. Ji, K.M.; Dai, H.X.; Deng, J.G.; Zang, H.J.; Arandiyani, H.; Xie, S.H.; Yang, H.G. 3DOM BiVO₄ supported silver bromide and noble metals: High-performance photocatalysts for the visible-light-driven degradation of 4-chlorophenol. *Appl. Catal. B Environ.* **2015**, *168–169*, 274–282. [[CrossRef](#)]
5. Gu, S.N.; Li, W.J.; Wang, F.Z.; Wang, S.Y.; Zhou, H.L.; Li, H.D. Synthesis of buckhorn-like BiVO₄ with a shell of CeOx nanodots: Effect of heterojunction structure on the enhancement of photocatalytic activity. *Appl. Catal. B Environ.* **2015**, *170–171*, 186–194. [[CrossRef](#)]
6. Wu, Q.; Chen, P.F.; Zhao, L.; Wu, J.; Qi, X.M.; Yao, W.F. Photocatalytic behavior of BiVO₄ immobilized on silica fiber via a combined alcohol-thermal and carbon nanofibers template route. *Catal. Commun.* **2014**, *49*, 29–33. [[CrossRef](#)]
7. Fan, H.M.; Jiang, T.F.; Li, H.Y.; Wang, D.J.; Wang, L.L.; Zhai, J.L.; He, D.Q.; Wang, P.; Xie, T.F. Effect of BiVO₄ crystalline phases on the photoinduced carriers behavior and photocatalytic activity. *J. Phys. Chem. C* **2012**, *116*, 2425–2430. [[CrossRef](#)]
8. Shen, Y.; Huang, M.L.; Huang, Y.; Lin, J.M.; Wu, J.H. The synthesis of bismuth vanadate powders and their photocatalytic properties under visible light irradiation. *J. Alloys Compd.* **2010**, *496*, 287–292. [[CrossRef](#)]
9. Sun, J.X.; Chen, G.; Wu, J.Z.; Dong, H.J.; Xiong, G.H. Bismuth vanadate hollow spheres: Bubble template synthesis and enhanced photocatalytic properties for photodegradation. *Appl. Catal. B Environ.* **2013**, *132–133*, 304–314. [[CrossRef](#)]
10. Dong, S.Y.; Feng, J.L.; Li, Y.K.; Hu, L.M.; Liu, M.L.; Wang, Y.F.; Pi, Y.Q.; Sun, J.Y.; Sun, J.H. Shape-controlled synthesis of BiVO₄ hierarchical structures with unique natural-sunlight-driven photocatalytic activity. *Appl. Catal. B Environ.* **2014**, *152–153*, 413–424. [[CrossRef](#)]
11. Ran, R.; McEvoy, J.G.; Zhang, Z. Synthesis and Optimization of Visible Light Active BiVO₄ Photocatalysts for the Degradation of RhB. *Int. J. Photoenergy* **2015**, *2015*, 612857. [[CrossRef](#)]
12. Kudo, A.; Omori, K.; Kato, H. A novel aqueous process for preparation of crystal form-controlled and highly crystalline BiVO₄ powder from layered vanadates at room temperature and its photocatalytic and photophysical properties. *J. Am. Chem. Soc.* **1999**, *121*, 11459–11467. [[CrossRef](#)]
13. Guo, M.; He, Q.; Wang, A.; Wang, W.; Fu, Z. A Novel, Simple and Green Way to Fabricate BiVO₄ with Excellent Photocatalytic Activity and Its Methylene Blue Decomposition Mechanism. *Crystals* **2016**, *6*, 81. [[CrossRef](#)]
14. Sarkar, S.; Chattopadhyay, K.K. Visible light photocatalysis and electron emission from porous hollow spherical BiVO₄ nanostructures synthesized by a novel route. *Phys. E* **2014**, *58*, 52–58. [[CrossRef](#)]
15. Dong, L.; Zhang, X.; Dong, X.; Zhang, X.; Ma, C.; Ma, H.; Xue, M.; Shi, F. Structuring porous “sponge-like” BiVO₄ film for efficient photocatalysis under visible light illumination. *J. Colloid Interface Sci.* **2013**, *393*, 126–129. [[CrossRef](#)]

16. Deebasree, J.P.; Maheskumar, V.; Vidhya, B. Investigation of the visible light photocatalytic activity of BiVO₄ prepared by sol gel method assisted by ultrasonication. *Ultrason. Sonochem.* **2018**, *45*, 123–132. [[CrossRef](#)] [[PubMed](#)]
17. Chen, S.H.; Jiang, Y.S.; Lin, H.Y. Easy Synthesis of BiVO₄ for Photocatalytic Overall Water Splitting. *ACS Omega* **2020**, *5*, 8927–8933. [[CrossRef](#)]
18. Xiao, B.C.; Lin, L.Y.; Hong, J.Y.; Lin, H.S.; Song, Y.T. Synthesis of a monoclinic BiVO₄ nanorod array as the photocatalyst for efficient photoelectrochemical water oxidation. *RSC Adv.* **2017**, *7*, 7547–7554. [[CrossRef](#)]
19. Yadav, A.A.; Hunge, Y.M.; Kang, S.W. Porous nanoplate-like tungsten trioxide/reduced graphene oxide catalyst for sonocatalytic degradation and photocatalytic hydrogen production. *Surf. Interfaces* **2021**, *24*, 101075. [[CrossRef](#)]
20. Li, G.Q.; Bai, Y.; Zhang, W.F. Difference in valence band top of BiVO₄ with different crystal structure. *Mater. Chem. Phys.* **2012**, *136*, 930–934. [[CrossRef](#)]
21. Yi, J.; Zhao, Z.Y.; Wang, Y.A.; Zhou, D.C.; Ma, C.S.; Cao, Y.C.; Qiu, J.B. Monophasic zircon-type tetragonal Eu_{1-x}Bi_xVO₄ solid-solution: Synthesis, characterization, and optical properties. *Mater. Res. Bull.* **2014**, *57*, 306–310. [[CrossRef](#)]
22. Zhou, B.; Zhao, X.; Liu, H.J.; Qu, J.H.; Huang, C.P. Synthesis of visible-light sensitive M-BiVO₄ (M=Ag, Co, and Ni) for the photocatalytic degradation of organic pollutants. *Sep. Purif. Tech.* **2011**, *77*, 275–282. [[CrossRef](#)]
23. Jiang, H.; Dai, H.; Meng, X.; Zhang, L.; Deng, J.; Liu, Y.; Au, C.T. Hydrothermal fabrication and visible-light-driven photocatalytic properties of bismuth vanadate with multiple morphologies and/or porous structures for methyl orange degradation. *J. Environ. Sci.* **2012**, *24*, 449–457. [[CrossRef](#)]
24. Liu, W.; Lai, S.Y.; Dai, H.; Wang, S.; Sun, H.; Au, C.T. Oxidative dehydrogenation of n-butane over mesoporous VO_x/SBA15 catalysts. *Catal. Lett.* **2007**, *113*, 147–154. [[CrossRef](#)]
25. Wang, G.; Ling, Y.; Lu, X.; Qian, F.; Tong, Y.; Zhang, J.Z.; Lordi, V.; Rocha Leao, C.; Li, Y. Computational and photoelectrochemical study of hydrogenated bismuth vanadate. *J. Phys. Chem. C* **2013**, *117*, 10957–10964. [[CrossRef](#)]
26. Jiang, H.-Q.; Endo, H.; Natori, H.; Nagai, M.; Kobayashi, K. Fabrication and photoactivities of spherical-shaped BiVO₄ photocatalysts through solution combustion synthesis method. *J. Eur. Ceram. Soc.* **2008**, *28*, 2955–2962. [[CrossRef](#)]
27. Hunge, Y.M.; Yadav, A.A.; Mohite, B.M.; Mathe, V.L.; Bhosale, C.H. Photoelectrocatalytic degradation of sugarcane factory wastewater using WO₃/ZnO thin films. *J. Mater. Sci. Mater. Electron.* **2018**, *29*, 3808–3816. [[CrossRef](#)]
28. Hunge, Y.M.; Yadav, A.A.; Mahadik, M.A.; Bulakhe, R.N.; Shim, J.J.; Mathe, V.L.; Bhosale, C.H. Degradation of organic dyes using spray deposited nanocrystalline stratified WO₃/TiO₂ photoelectrodes under sunlight illumination. *Opt. Mater.* **2018**, *76*, 260–270. [[CrossRef](#)]
29. Chang, W.S.; Li, Y.C.M.; Chung, T.W.; Lin, Y.S.; Huang, C.M. Toluene decomposition using silver vanadate/SBA-15 photocatalysts: DRIFTS study of surface chemistry and recyclability. *Appl. Catal. A Gen.* **2011**, *407*, 224–230. [[CrossRef](#)]
30. Pan, G.T.; Huang, C.M.; Peng, P.Y.; Yang, T.C.K. Nano-scaled silver vanadates loaded on mesoporous silica: Characterization and photocatalytic activity. *Catal. Today* **2011**, *164*, 377–383. [[CrossRef](#)]
31. Ameen, S.; Akhtar, M.S.; Nazim, M.; Shin, H.S. Rapid photocatalytic degradation of crystal violet dye over ZnO flower nanomaterials. *Mater. Lett.* **2013**, *96*, 228–232. [[CrossRef](#)]
32. Hunge, Y.M.; Yadav, A.A.; Khan, S.; Takagi, K.; Suzuki, N.; Teshima, K.; Terashima, C.; Fujishima, A. Photocatalytic degradation of bisphenol A using titanium dioxide@nanodiamond composites under UV light illumination. *J. Colloid Interf. Sci.* **2021**, *582*, 1058–1066. [[CrossRef](#)] [[PubMed](#)]
33. Hunge, Y.M.; Yadav, A.A.; Dhodamani, A.G.; Suzuki, N.; Terashima, C.; Fujishima, A.; Mathe, V.L. Enhanced photocatalytic performance of ultrasound treated GO/TiO₂ composite for photocatalytic degradation of salicylic acid under sunlight illumination. *Ultrason. Sonochem.* **2020**, *61*, 104849. [[CrossRef](#)] [[PubMed](#)]
34. Yadav, A.A.; Hunge, Y.M.; Kulkarni, S.B. Synthesis of multifunctional FeCO₂O₄ electrode using ultrasonic treatment for photocatalysis and energy storage applications. *Ultrason. Sonochem.* **2019**, *58*, 104663. [[CrossRef](#)] [[PubMed](#)]
35. Hunge, Y.M.; Yadav, A.A.; Kulkarni, S.B.; Mathe, V.L. A multifunctional ZnO thin film based devices for photoelectrocatalytic degradation of terephthalic acid and CO₂ gas sensing applications. *Sens. Actuators B Chem.* **2018**, *274*, 1–9. [[CrossRef](#)]
36. Hunge, Y.M.; Yadav, A.A.; Mathe, V.L. Oxidative degradation of phthalic acid using TiO₂ photocatalyst. *J. Mater. Sci. Mater.* **2018**, *29*, 6183–6187. [[CrossRef](#)]
37. Kathiresan, G.; Vijayakumar, K.; Sundarajan, A.P.; Kim, S.H.; Adaikalam, K. Photocatalytic degradation efficiency of ZnO, GO and PVA nanoadsorbents for crystal violet, methylene blue and trypan blue dyes. *Optik* **2021**, 166671. [[CrossRef](#)]
38. Puneetha, J.; Kottam, N.; Rathna, A. Investigation of photocatalytic degradation of crystal violet dye and its co relation with bandgap in ZnO and ZnO/GO nanohybrid. *Inorg. Chem. Commun.* **2021**, *125*, 108460.
39. Sajid, M.M.; Amin, N.; Shad, N.A.; Sadaf Bashir Khan, S.B.; Javed, Y.; Zhangd, Z. Hydrothermal fabrication of monoclinic bismuth vanadate (m-BiVO₄) nanoparticles for photocatalytic degradation of toxic organic dyes. *Mater. Sci. Eng. B* **2019**, *242*, 83–89. [[CrossRef](#)]
40. Ju, Y.; Fang, J.; Liu, X.; Xu, Z.; Ren, X.; Sun, C.; Yang, S.; Ren, Q.; Ding, Y.; Yu, K.; et al. Photodegradation of crystal violet in TiO₂ suspensions using UV-V is irradiation from two microwave-powered electrodeless discharge lamps (EDL-2): Products, mechanism and feasibility. *J. Hazard. Mater.* **2011**, *185*, 1489–1498. [[CrossRef](#)]
41. Yadav, A.A.; Hunge, Y.M.; Mathe, V.L.; Kulkarni, S.B. Photocatalytic degradation of salicylic acid using BaTiO₃ photocatalyst under ultraviolet light illumination. *J. Mater. Sci. Mater.* **2018**, *29*, 15069–15073. [[CrossRef](#)]